

Searching for Cosmic Strings in New Observational Windows

Robert H. Brandenberger^{1,*}

¹*Physics Department, McGill University, 3600 University Street, Montreal, QC, H3A 2T8, Canada*

Cosmic strings are predicted in many models beyond the Standard Model of particle physics. In models which admit strings, a network of strings will inevitably be formed in a phase transition in the early universe and will persist to the present time. Strings leave behind distinctive features in cosmology. Searching for these signatures in new observational windows provides a way to constrain particle physics at the high energy scale and is thus complementary to searches for new physics at the low energy end, for example at the LHC. Specifically, I will discuss signatures of cosmic strings in cosmic microwave background polarization maps and in 21cm redshift surveys.

PACS numbers: 98.80.Cq

I. INTRODUCTION

Cosmic strings [1] are linear topological defects which arise in a range of relativistic quantum field theories (for reviews see e.g [2]). Good analogs of cosmic strings are vortex lines in superfluids and superconductors. Line defects in crystals can be viewed as another analog system. Cosmic strings form lines of trapped energy density, and this energy density can curve space-time and have important effects in cosmology [3].

Cosmic strings are predicted to form in many particle physics models beyond the Standard Model. In particular, they are predicted to form at the end of inflation in many inflationary models, e.g. supergravity models [4] and brane inflation models [5]. Cosmic strings may also survive as cosmic superstrings in alternatives to inflation such as “String Gas Cosmology” [6]. The key point for cosmology is that in any field theory model which admits cosmic string solutions, a network of strings inevitably forms at some point during the early universe [7], and it persists to the present time. Hence, the detection of cosmic strings would give us information about particle physics at very high energy scales.

Since cosmic strings are relativistic objects, a straight string is described by one number, namely its mass per unit length μ which also equals its tension, or equivalently by the dimensionless number $G\mu$, where G is Newton’s gravitational constant (we are using units in which the speed of light is $c = 1$). In simple quantum field theory models the tension is related to the energy scale η at which the strings are formed via $\mu \sim \eta^2$ (see the following section for a more precise discussion). The cosmological signatures of strings are thus more substantial for larger values of μ which implies larger values of the energy scale η . Hence, searching for cosmological signatures of strings is a tool to probe particle physics beyond the Standard Model at the highest energy scales (as opposed to accelerator experiments like the LHC which probe new physics at low energy scales).

In fact, current limits on cosmic strings already [8] provide a constraint

$$G\mu < 1.5 \times 10^{-7} \quad (1)$$

which rules out certain Grand Unified particle physics models with very high scale symmetry breaking. This limit comes from the observational upper bound on the contribution of cosmic strings to the angular power spectrum of cosmic microwave background (CMB) anisotropies obtained by combining the results of the WMAP satellite [9] with those of the South Pole Telescope [10] (see also [11] for a comparable limit obtained by combining results from WMAP and from the Atacama Cosmology Telescope [12], and [13] for earlier limits).

Given the constraints on particle physics models which can be derived from current observations, it is of great interest to try to improve the observational upper bounds on the cosmic string tension since this will allow us to constrain high energy scale particle physics models more strongly than what is possible today.

Cosmic strings can also produce many good things for cosmology in addition to contributing to cosmological structure formation. Cosmic strings may play a role in baryogenesis (see e.g. [14]). Certain types of strings can provide a mechanism for the production [15] of seed magnetic fields which are coherent on galactic scales¹. Cusps on cosmic string loops can also yield a contribution to ultra-high-energy cosmic rays [16, 17]. Finally, cosmic string loops may assist in the assembly of the large mass concentrations required to seed super-massive black holes.

For all of the above reasons it would thus be wonderful to have evidence for the existence of cosmic strings in nature. The search for cosmic strings is therefore of great interest independent of whether the search in fact finds

*Electronic address: rhb@physics.mcgill.ca

¹ The challenge for particle physics models of magnetogenesis is to obtain the observed coherence length since microphysics typically produces coherence lengths which are much too small. In the case of cosmic string seeds, the increase of the comoving curvature radius of the long strings provides the mechanism of obtaining a large magnetic field coherence length.

signals of cosmic strings. If it does, then we will have discovered something completely new in the universe. If it does not, then we will have derived tighter constraints on particle physics at very high energy scales.

In this talk I will review recent work on signatures of cosmic strings in new observational windows. Up to the present time, the tightest and most robust constraints on the cosmic string tension have come from analyses of CMB temperature maps. Here, I will focus on the signatures of strings in CMB polarization maps and 21cm redshift surveys, two emerging windows to explore the cosmos.

The main points to take away from this talk are the following. Firstly, cosmic strings lead to nonlinearities already at very high redshifts. Hence, the signatures of cosmic strings are more pronounced at higher than at lower redshifts where they are masked by the nonlinearities produced by the Gaussian density fluctuations which must be present and which dominate the total power spectrum of cosmological perturbations. Secondly, cosmic strings lead to perturbations which are highly non-Gaussian and which predict specific geometrical patterns in position space. By computing a power spectrum, information about these patterns are lost. Hence, tighter limits on the cosmic string tension can be obtained if we analyze the data in position space. Thirdly, 21cm redshift surveys appear to be an ideal window to search for cosmic string signatures [18].

The outline of this talk is as follows. We first present a brief review of the basics of cosmic strings. In Section 3 we introduce the two main mechanisms which will play a role in determining the cosmic string signals in observations, namely the Kaiser-Stebbins [19] (see also [20]) lensing effect and the cosmic string wake [21]. We also briefly review the well-known resulting signal of strings in CMB temperature maps. The key sections of this talk are Sections 4 and 5. In the first, we discuss the signal of a long straight cosmic string in CMB polarization maps, and in the second we turn to the signal in 21cm redshift surveys.

II. COSMIC STRING REVIEW

In a class of relativistic quantum field theories, cosmic strings form after a phase transition in the early universe during which an internal symmetry in field space is spontaneously broken. Let us consider a simple toy model involving a complex scalar field ϕ with potential

$$V(\phi) = \frac{\lambda}{4}(|\phi|^2 - \eta^2)^2 \quad (2)$$

where η is the vacuum expectation value of the modulus of ϕ and λ is a coupling constant.

To determine whether a particular field theory admits cosmic string solutions or not, the key concept is that of the *vacuum manifold* \mathcal{M} , the set of field values which

minimizes the potential. In the above example \mathcal{M} is homotopically equivalent to the circle S^1 .

In thermal equilibrium, the potential obtains finite temperature corrections [22, 23] (see e.g. [24] for a review). Specifically, there is an extra contribution

$$\Delta V_T(\phi) \sim T^2 |\phi|^2, \quad (3)$$

where T is the temperature. Hence, there is a critical temperature T_c above which the lowest potential energy state is $\phi = 0$ and the field symmetry (rotation in the complex field plane) is unbroken. Thus, in the early universe the average value of ϕ at each point in space will be $\phi = 0$, but as the universe cools below the temperature T_c this state becomes unstable and at each point in space ϕ will want to roll down the potential to take on a value in \mathcal{M} .

The key point is [7] that by causality there can be no correlation between the field values in \mathcal{M} which are taken on at points in space which are out of causal contact, i.e. which are further apart than the Hubble distance t . Hence, there is a probability of order 1 that the field values in \mathcal{M} evaluated for a loop \mathcal{C} in space of radius t will form an incontractible loop in \mathcal{M} . This implies that there must be a point in space on any disk bounded by \mathcal{C} where $\phi = 0$. Around these points there is trapped potential and spatial gradient energy.

Energy minimization arguments make it obvious that the distinguished points on different disks (with the same boundary) form part of a line. This line is the cosmic string. It is a line of points with $\phi = 0$ surrounded by a tube of trapped energy. The width w of the tube is determined by minimizing the sum of potential and spatial gradient energy, leading to the result

$$w = \lambda^{-1/2} \eta^{-1} \quad (4)$$

such that the resulting mass per unit length μ is independent of the coupling constant:

$$\mu = \eta^2 \quad (5)$$

(up to numerical factors independent of λ).

To recap, causality tells us that at the symmetry breaking phase transition at time $t = t_c$ a network of cosmic strings will form in any field theory model which admits cosmic string solutions. Cosmic strings are closed - they cannot have ends. Hence, they are either string loops or infinite in length. Note that causality in fact ensures that (in an infinite space) strings of infinite length will be formed. A way to picture the network of strings is as a random walk with typical curvature radius $\xi(t)$ which is bounded from above by the Hubble length t .

The same causality argument which is used to predict the formation of strings can be used to show that the network of strings will survive at all times $t > t_c$, including the present time. Hence, cosmic strings formed in the very early universe will lead to signatures which can be searched for in current cosmological observations.

We will work in terms of a one-scale model [25] of the cosmic string distribution which is given by the correlation length $\xi(t)$ which describes both the mean curvature radius and the separation of the “long” strings (“long” meaning with length greater than t). Kibble’s causality argument tells us that $\xi(t) < t$. Dynamical arguments show that $\xi(t)$ cannot be much smaller than t . The argument is as follows: cosmic strings are relativistic objects. If the curvature radius is smaller than t , then the strings will move with relativistic speed. Hence, intersections of strings will occur. It can be shown [26] that unless the relative speed of two intersecting string segments is extremely close to the speed of light, then the string segments will not cross, but they will intersect and exchange ends. In this way, the long strings can form string loops, which in turn oscillate and decay by emitting gravitational radiation. This process is described by a Boltzmann equation (see e.g. [2]) from which it follows that if $\xi(t) \ll t$ then $\xi(t)/t$ will increase, and that there will be a dynamical fixed point *scaling solution* with

$$\xi(t) \sim t. \quad (6)$$

The approach to a scaling solution has been confirmed in a series of numerical simulations [27]. The process of long string intercommutation leaves behind a distribution of cosmic string loops which also achieves a scale-invariant form. We will not discuss this issue since we will focus on the cosmological signatures of the long strings.

Since cosmic strings carry energy, they can gravitate and produce cosmological signals. This was first pointed out in [3]. In the early 1980s cosmic strings were studied as an alternative to cosmological inflation [25]. Cosmic string formation produces entropy fluctuations on super-Hubble scales which then seed a curvature fluctuation which grows on super-Hubble scales. Such fluctuations are called “active”. They are also “incoherent” meaning that there are no phase correlations in phase space between different Fourier modes [28]. Hence, although cosmic strings predict a spectrum of density fluctuations which is scale-invariant and hence an angular power spectrum of CMB anisotropies which is also scale-invariant on large angular scales [29], the acoustic oscillations which are characteristic of models like inflation where a scale-invariant spectrum of adiabatic fluctuations are generated whose amplitude remains constant on super-Hubble scales are absent [28]. Once the acoustic oscillations were discovered by various experiments such as the Boomerang experiment [30], interest in cosmic strings collapsed.

However, given the realization that cosmic strings are produced after inflation in many particle physics models, interest in searching for observational signatures of cosmic strings as a supplementary (not main) source of structure in the universe has increased. The search for strings in the cosmos is emerging as a promising way to probe physics at energy scales much larger than those that can ever be reached in terrestrial accelerators, as already mentioned above. Independent of whether strings

are in fact discovered or the bounds on the existence of strings are improved we will have learned a lot about particle physics.

III. KAISER-STEBBINS EFFECT AND COSMIC STRING WAKES

In this talk I will focus on gravitational effects of cosmic strings. These are based on two main “actors”, firstly the *Kaiser-Stebbins* lensing effect [19, 20], and secondly the existence of *string wakes* [21].

The string lensing effect is based on the fact that a long straight cosmic string with equal tension and energy per unit length leads to a conical structure of space perpendicular to the string [31]. Unwrapping the cone onto a plane leads to a “deficit angle”

$$\alpha = 8\pi G\mu. \quad (7)$$

If we now consider a cosmic string with transverse velocity v and associated relativistic gamma factor $\gamma(v)$, then if we look at the CMB in direction of the string (see Fig. 1), then photons passing on the two sides of the string are observed with a relative Doppler shift

$$\frac{\delta T}{T} = 8\pi\gamma(v)vG\mu. \quad (8)$$

This leads to a line discontinuity in the CMB sky, the linear direction corresponding to the projection of the tangent vector of the string onto our last light cone [19, 20].

Given a scaling distribution of strings, each string which intersects our past light cone will lead to a line discontinuity in the CMB sky. As shown in [32], for strings formed at a phase transition at time t_c in the early universe (as opposed to idealized strings being present at all times), the deficit angle at time t has finite depth $d(t)$, namely

$$d(t) \simeq (t - t_c) \simeq t \quad (9)$$

for $t \gg t_c$. Hence, the signature of an individual string in the sky corresponds to a rectangle in the sky with the above value of δT . The dimensions of the rectangle are the angles given by the comoving distances corresponding to length $c_1 t$ and depth t , where c_1 is a constant of order 1.

We will be making use of a toy model for the (long) cosmic string scaling first introduced in [33] and widely used since then in cosmic string research. We replace the infinite string network at time t by a set of straight string segments of length $c_1 t$ whose center of mass positions, tangent vectors and velocity vectors are randomly distributed and uncorrelated. These string segments live for one Hubble expansion time (the average time between string intercommutations). In the subsequent Hubble time steps there are new string segments with larger length whose centers, tangent and velocity vectors are

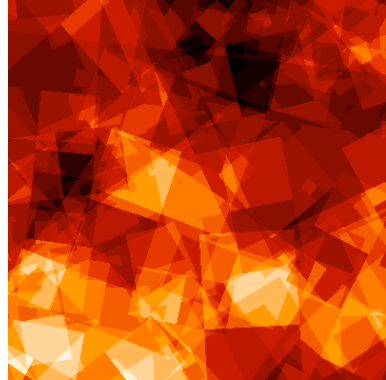
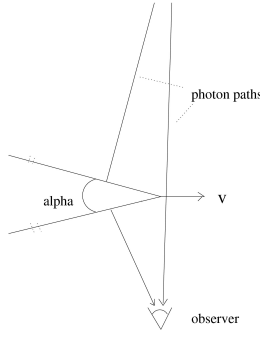


FIG. 1: Sketch of the geometry of space perpendicular to a long straight string segment. Space is conical which corresponds to a deficit angle in the plane. If the string is moving with velocity v in a direction transverse to the direction of the string, then photons passing on different sides of the string are measured with a relative Doppler shift. This is the Kaiser-Stebbins effect.

assumed to be uncorrelated with those of the string segments in the previous Hubble time step. As a reflection of the scaling of the string network, we consider a fixed number N per string segments in each Hubble volume. The number N can be determined by comparing with numerical simulations. Causality tells us that $N \geq 1$. Numerical simulations give values of the order $N \sim 10$ [27].

String segments in each Hubble time step contribute to the total Kaiser-Stebbins effect. String segments in the first Hubble time step after recombination are the most numerous. The size in the sky of the corresponding temperature patches is about one degree. Strings from later Hubble time steps are less numerous but larger (see Fig. 2).

To identify the signal of cosmic strings in CMB temperature maps, good angular resolution is more important than full sky coverage. Hence, experiments such as SPT and ACT will yield better limits than even the Planck satellite.

The distinctive edges in CMB temperature maps produced by strings are washed out in the angular power spectrum. Hence, tighter limits can be set on the string tension by analyzing the CMB maps in position space using edge detection algorithms rather than by simply computing a power spectrum. Specifically, by using a numerical implementation of the Canny edge detection algorithm [34] it appears that a bound one order of magnitude stronger than the current bound might be achiev-

FIG. 2: CMB anisotropy map for a $10^\circ \times 10^\circ$ patch of the sky at $1.5'$ resolution (the specifications are chosen to be comparable to those of the SPT and ACT telescopes - in fact both of these telescopes map a larger fraction of the sky) in a model in which the fluctuations are given by a scaling distribution of cosmic strings. The color coding indicates the amplitude of the temperature anisotropy.

able by using data from the SPT telescope [35] (see also [36, 37] for initial work on applying the Canny algorithm to CMB maps). The projected bound is

$$G\mu \leq 2 \times 10^{-8}. \quad (10)$$

The second main “actor” in the story presented here is the cosmic string wake [21]. Consider a long straight string segment moving through the uniform matter distribution of the early universe. From the point of view of a point behind the moving string, it appears as though matter acquires a velocity perturbation

$$\delta v = 4\pi v\gamma(v)G\mu \quad (11)$$

from above and below towards the plane behind the mov-

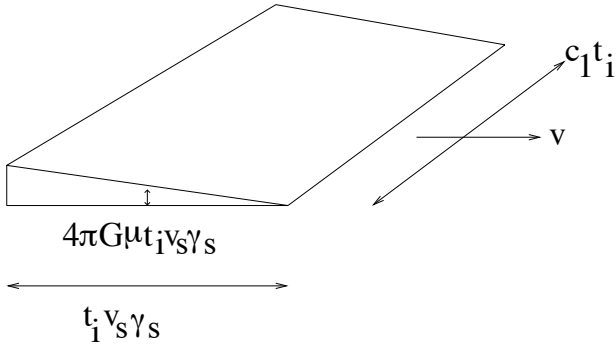


FIG. 3: Geometry of a cosmic string wake. Such a wake is extended in the plane spanned by the direction tangential to the string segment and by the velocity vector, while its initial size perpendicular to this plane is thin. In the figure, v_s is the string velocity v , and γ_s is its related gamma factor.

ing string. This in turn leads to a wedge-shaped overdensity (twice the background density) behind the string. This is the *wake*.

Working again in the context of the toy model of [33], each string segment in each Hubble expansion time generated a wake. Consider a string at time t_i . The physical dimension of the induced wake at the time t_i will be

$$c_1 t_i \times v \gamma(v) t_i \times 4\pi v \gamma(v) G \mu t_i, \quad (12)$$

where the first factor is the size along the tangent vector of the string, the second factor is the depth (in direction opposite to the string motion), and the third factor is the mean width. At the leading edge (the instantaneous location of the string), the width of the wake is zero, whereas at the trailing edge (the initial position of the string segment) the width is twice the mean width w .

Once formed, a wake will grow in thickness via gravitational accretion. This process can be studied using the Zel'dovich approximation [38]. The idea is to consider a shell of matter which is located initially (at the time t_i when the wake is laid down) at a physical height $h(t_i) = a(t_i)q$ above the center of the wake. The quantity q is the initial comoving height. As a consequence of the gravitational pull of the matter overdensity in the wake, a comoving displacement $\psi(t)$ gradually builds up (where $\psi(t_i) = 0$). The physical height at time $t > t_i$ then can be written as

$$h(q, t) = a(t)(q - \psi),$$

where $a(t)$ is the cosmological scale factor. The time evolution of the height is then determined via Newtonian gravity

$$\ddot{h} = -\frac{\partial \Phi}{\partial h}, \quad (13)$$

where Φ is the Newtonian gravitational potential which is determined via the Poisson equation in terms of the mass overdensity. We then calculate the value $q(t)$ (which we

call $q_{nl}(t, t_i)$) for which the shell is “turning around” at time t , i.e.

$$\dot{h}(q(t), t) = 0. \quad (14)$$

After turnaround, the shell will virialize at a physical height which is half the turnaround height ² This virialized region forms the wake. The result of a straightforward calculation shows that (in agreement with what follows from linear perturbation theory), the comoving height of the wake grows linearly in the scale factor, i.e.

$$q_{nl}(t, t_i) = \frac{a(t)}{a(t_i)} \frac{24\pi}{5} v \gamma(v) G \mu (z(t_i) + 1)^{-1/2} t_0, \quad (15)$$

where the expression on the right hand side is the ratio of scale factors multiplying the initial comoving width of the wake (modulo a factor of order 1). Note that $z(t)$ is the cosmological redshift. In the context of cosmic strings this analysis was originally done in [40] (accretion onto loops) and [41] (accretion onto wakes).

Since the turnaround height itself is half the height the shell would have if it were simply to expand with the Hubble flow, the resulting overdensity in the wake is a factor of 4. Note that for accretion onto a string loop, the resulting overdensity is 64 since there is contraction in all three spatial directions (see e.g. [42]).

Let us end this section with a couple of comments. First of all, the planar dimensions of the wake will retain constant comoving size. Secondly, there is an important difference between the lensing signal due to string segments and the wake signal. Since the string segment only lives for one Hubble expansion time, only strings whose finite time world sheet intersects the past light cone lead to an observable signal. On the other hand, wakes persist even after the string segment which has seeded them has decayed. Hence, all string segments within the past light cone lead to observable wake signals. In the following, it is signals due to wakes which will be discussed.

IV. SIGNATURES OF COSMIC STRINGS IN CMB POLARIZATION

When primordial CMB quadrupole radiation scatters off of a gas cloud, the residual free electrons in the cloud lead to polarization. Wakes are regions of enhanced density, and hence also of enhanced free electron density. Photons emitted at the time of recombination acquire extra polarization when they pass through a string wake. It is this signal which we study here [43].

There are two polarization modes - E and B modes. A Gaussian random field of density fluctuations leads to pure E-mode polarization. In contrast, cosmic string

² Note that this picture of cosmic string wake growth has been confirmed by an Eulerian hydro simulation [39].

wakes lead to a statistically equal distribution of E and B-mode polarization. The reason for the generation of a B-mode component is that there is a distinguished vector given by the normal vector to the wake. This vector is independent of the CMB quadrupole vector.

The amplitude P of the polarization signal depends on the column density of free electrons which the CMB photons encounter when they cross the wake. If t is the time when the photons are passing through the wake, the column density is proportional to the residual ionization fraction $f(t)$ at time t , the number density of baryons and the width of the wake. The value of P is then determined by multiplying the result with the scattering cross section σ_T and the amplitude Q of the CMB quadrupole. The result is (see [43] for details):

$$\frac{P}{Q} \simeq \frac{24\pi}{25} \left(\frac{3}{4\pi}\right)^{1/2} \sigma_T f(t) G \mu v \gamma(v) \times \Omega_B \rho_c(t_0) m_p^{-1} t_0 (z(t) + 1)^2 (z(t_i) + 1)^{1/2}, \quad (16)$$

where t_i is the time when the wake is laid down, Ω_B is the fraction of the total energy density which is in baryons, and $\rho_c(t_0)$ is the critical energy density (energy density of a spatially flat universe) at the present time t_0 .

Note that the induced polarization increases as the wake formation time decreases. This is because early wakes have had time to accrete more matter and are thicker than late wakes. The value of P also increases as $z(t)$ increases. This is because the density in a wake is larger at earlier times than later ones. Inserting the value of the constants appearing above and evaluating the result in units of the characteristic values $z(t) + 1 = z(t_i) + 1 = 10^3$ we obtain

$$\frac{P}{Q} \sim f(t) G \mu v \gamma(v) \Omega_B \left(\frac{z(t) + 1}{10^3}\right)^2 \left(\frac{z(t_i) + 1}{10^{1/2}}\right)^3 10^7. \quad (17)$$

The residual ionization fraction drops off after recombination to a value of between 10^{-5} and 10^{-4} (see e.g. [44]), but increases again at the time of reionization to a value of order unity. However, as can be seen from (17), the predicted CMB polarization has an amplitude which is suppressed by either $f(t)$ for times t between recombination and reionization, or by the square of $(z(t) + 1)/10^3$ for times after reionization.

In spite of the small amplitude of the signal, the string-induced polarization may still be detectable because of the specific geometry of the signal in position space: a cosmic string wake leads to a rectangular region in the sky with extra polarization with almost uniform polarization axis and with an amplitude which is increasing monotonically from the leading edge of the wake (where the string is located) to the trailing edge (where the string was at the time of wake formation), and because statistically an equal amount of E-mode and B-mode polarization is generated.

In this context, I wish to comment on the statement which is often heard that “B-mode polarization is the

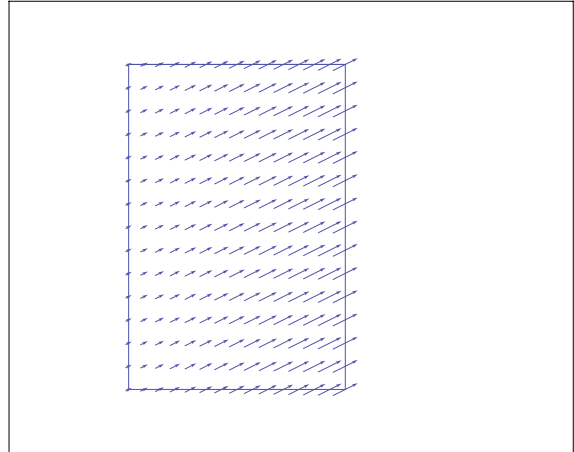


FIG. 4: The CMB anisotropy polarization pattern (direction and magnitude indicated by the arrows) produced by a cosmic string wake. For a wake produced close to the time of recombination, the angular size is about one degree.

“holy grail of inflation”³. What is usually meant by this statement is that B-mode polarization is predicted in inflationary models from the spectrum of gravitational waves which inflation generates. Thus, it is claimed that the detection of B-mode polarization will be a signal of the gravitational waves which inflation predicts. However, as we have shown above, cosmic strings predict direct B-mode polarization independent of gravitational waves. Thus, it is not correct to interpret a potential detection of B-mode polarization as being due to gravitational waves.

Secondly, there are sources of gravitational waves which generically lead to a higher amplitude of such waves than what is obtained in the simplest single field slow-roll inflation models. Specifically, the cosmic string loops which are inevitably produced via the dynamics of the scaling network of long strings will oscillate and decay by emitting gravitational waves. Thus, a detection of gravitational waves (via B-mode polarization or other means) is more likely to be a signal of something different from inflation.

There is, in fact, an interesting twist to the story: If B-mode polarization is discovered and shown to be due to gravitational waves, and a blue spectrum (more power on shorter wavelengths) is measured, then this would rule out these gravitational waves as being due to inflation. Instead, it would be the confirmation of an effect first predicted in the context of superstring theory, namely the spectrum induced in the string gas alternative to inflationary cosmology [46].

In conclusion, B-mode polarization can be viewed as the “holy grail” of early universe cosmology, but not as the “holy grail” of inflation.

³ The following paragraphs are based on [45].

V. SIGNATURES OF COSMIC STRINGS IN 21CM SURVEYS

The 21cm redshift survey technique is emerging as a promising tool to probe cosmology, in particular the high redshift universe, the universe during the “dark ages” (i.e. before the onset of star formation).

The physics is the following: after the time of recombination but before reionization the baryonic matter in the universe is mostly in the form of neutral hydrogen. Neutral hydrogen has a hyperfine transition line at a frequency corresponding for 21cm. If we consider the primordial CMB radiation passing through a gas cloud, then the spectrum at the rest frame frequency of 21cm is changed by excitation or de-excitation of the hyperfine transition. The primordial 21cm photons can be absorbed by the gas cloud. In turn, a hot gas cloud will emit 21cm photons. Whether the net effect is an absorption or emission effect depends on the temperature of the gas cloud.

Any gas cloud which intersects our past light cone at some time between recombination and the present time will yield a 21cm signal. If the time of intersection corresponds to a redshift $z(t)$, then the emission / absorption signal will be seen at the redshifted wavelength

$$\lambda(t) = (z(t) + 1)\lambda_0, \quad (18)$$

where λ_0 is 21cm. Hence, 21cm redshift surveys provide a means for mapping the distribution of baryonic matter as a function of redshift, including at times before the onset of star formation.

Cosmic string wakes are nonlinear density perturbations present at arbitrarily early times with a distinctive geometric pattern in position space. Thus, as realized in [18], (see also [47] for early work on cosmic strings and 21cm redshift surveys), cosmic strings predict striking signals, in particular at redshifts before reionization.

Let us begin this section with some basic equations required to compute the 21cm signal (see [48] for a comprehensive review of 21cm cosmology). Let us consider primordial CMB photons passing through a gas cloud at redshift $z(t)$. Then the brightness of the 21cm radiation emerging from the gas cloud is

$$T_b(\nu) = T_S(1 - e^{-\tau_\nu}) + T_\gamma(\nu)e^{-\tau_\nu}, \quad (19)$$

where T_S is the “spin temperature” of the hydrogen atoms in the gas cloud, and T_γ is the temperature of the CMB photons before entering the gas cloud. The quantity τ_ν is the optical depth at the frequency being considered. The second term in (19) describes the absorption of the primordial CMB photon due to excitation of the hydrogen atoms, the first term gives the contribution due to de-excitation of the hydrogen atoms.

The spin temperature introduced above determines the excitation level of the hydrogen atoms. It is related to the gas temperature in the wake and to the CMB tem-

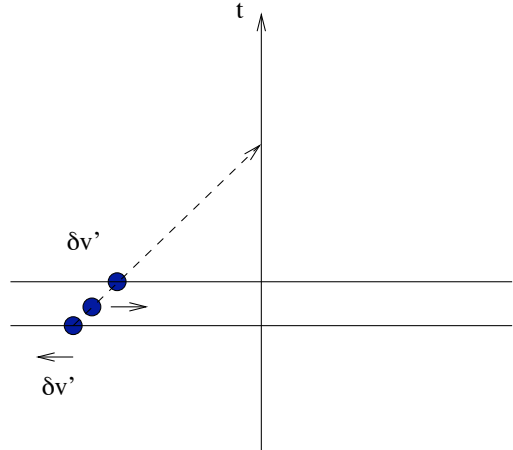


FIG. 5: Space-time sketch (space as horizontal axis and time in vertical direction) showing 21cm photons emitted from a string wake. Looking in a fixed direction in the sky, photons from the wake will undergo different amount of cosmological redshift and will hence arrive with a frequency dispersion.

perature via a collision coefficient x_c :

$$T_S = \frac{1 + x_c}{1 + x_c T_\gamma / T_K} T_\gamma. \quad (20)$$

The relative brightness temperature measured by the observer today is

$$\delta T_b(\nu) = \frac{T_b(\nu) - T_\gamma(\nu)}{1 + z}, \quad (21)$$

where the denominator is due to the redshifting of the temperatures between the time when the gas cloud intersects our past light cone and the present time.

Let us now turn to the application to cosmic string wakes. Fig. 5 presents a sketch of 21cm photons from a string wake. As indicated, there will be a frequency dispersion caused by the different times the photons are emitted. Its magnitude is proportional to the width of the wake and is given by

$$\frac{\delta\nu}{\nu} = 2\sin(\theta)\tan(\theta)Hw, \quad (22)$$

where H is the Hubble expansion rate, w is the wake width, and θ is the angle between the perpendicular to the plane of the wake and the line of sight towards us.

The optical depth for 21cm photons passing through the wake is (in units where $c = \hbar = k_B = 1$)

$$\tau_\nu = \frac{3A_{10}}{4\nu^2} \left(\frac{\nu}{T_S}\right) \frac{N_{HI}}{4} \phi(\nu), \quad (23)$$

where N_{HI} is the column number density of hydrogen atoms, A_{10} is the spontaneous emission coefficient of the 21cm transition, and $\phi(\nu)$ is the line profile

$$\phi(\nu) = \frac{1}{\delta\nu} \text{ for } \nu \in [\nu_{10} - \frac{\delta\nu}{2}, \nu_{10} + \frac{\delta\nu}{2}]. \quad (24)$$

Note that the width of the string wake (and hence the dependence on $G\mu$) cancels out between the column density and the line profile. This will lead to the relative brightness temperature signal being independent of the string tension.

To determine the relative brightness temperature, we also need to know the spin temperature of the hydrogen gas inside the wake. This is in turn determined (20) from the kinetic temperature of the wake. Assuming that the kinetic temperature is obtained via thermalization from the kinetic energy acquired during the Zel'dovich collapse of the wake leads to the result [18]

$$T_K \simeq [20 \text{ K}] (G\mu)_6^2 (v\gamma(v))^2 \frac{z_i + 1}{z + 1}, \quad (25)$$

where $(G\mu)_6$ is the value of $G\mu$ in units of 10^{-6} , z_i is the redshift of wake formation and z is the redshift at which the wake intersects the past light cone.

Inserting this result (25) into the expression for the 21cm brightness temperature (19) yields the following relative brightness temperature

$$\delta T_b(\nu) = [0.07 \text{ K}] \frac{x_c}{1 + x_c} \left(1 - \frac{T_\gamma}{T_K}\right) (1 + z)^{1/2} \quad (26)$$

whose amplitude is of the order

$$\delta T_b(\nu) \sim 200 \text{ mK} \text{ for } z + 1 = 30 \quad (27)$$

(we have taken the redshift of emission from the wake to be larger than the redshift of reionization so that we do not have to bother about nonlinearities from the Gaussian fluctuations).

The amplitude of the cosmic string-induced 21cm signal is thus very large. Whether the signal is in emission or absorption depends on which of T_K or T_γ is larger. In the former case (low redshifts) we have an emission signal, in the latter case it is a signal in absorption⁴. The transition between emission and absorption takes place when

$$(G\mu)_6^2 \simeq 0.1 (v\gamma(v))^{-2} \frac{(z + 1)^2}{z_i + 1}. \quad (28)$$

For values of $G\mu$ which are comparable or lower than the current upper bound, the signal is thus more likely to be in absorption rather than in emission.

Wakes formed after the time of recombination t_{rec} intersect the past light cone over a large area in the sky (comparable or greater to a square degree). Each wake will produce a signal in the form of a thin wedge in three dimensional redshift survey space. The leading edge of the wedge (where the cosmic string segment is located at the final time) corresponds to a later time and hence to

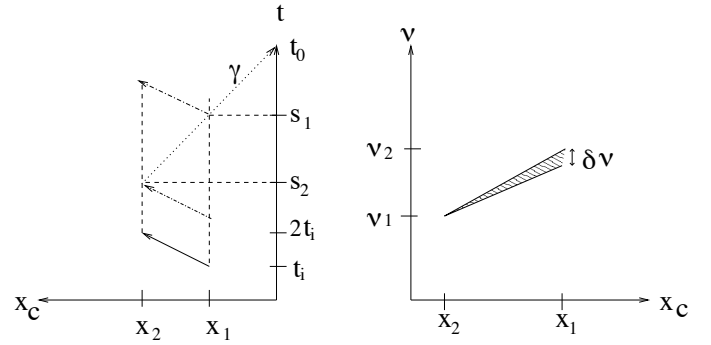


FIG. 6: Geometry of the 21cm signal of a cosmic string wake. On the left is a space-time sketch (horizontal axis being comoving spatial coordinates and vertical axis being conformal time) of the string wake which is laid down at time t_i . The string segment “lives” until the time $2t_i$. Its initial position is x_1 , its final position x_2 . The string wake extends in comoving coordinates from x_1 to x_2 . Its thickness at x_1 vanishes and is maximal at x_2 . The time t_0 is the present time. Our past light cone (indicated by the line labelled γ) intersects the string wake. For the configuration shown, the past light cone intersects the leading (thin) edge of the wake earlier than the trailing edge. Hence, 21cm photons from the leading edge are redshifted more than those from the trailing edge. This gives rise to a characteristic wedge of extra 21cm absorption / emission due to the string wake in 21cm redshift maps. This wedge is sketched on the left of the figure, a sketch in which the horizontal axis is the same comoving spatial coordinate as in the left sketch, and the vertical axis is the detected 21cm frequency.

a frequency which has undergone less frequency redshift. Thus, the two “large” dimensions of the wedge are not exactly perpendicular to the frequency axis. The geometry is illustrated in Fig. 6.

Whereas the amplitude of the brightness temperature signal at a fixed point inside the wedge does not depend to a first approximation on $G\mu$, the width of the wedge does depend on it. The relative width is given by

$$\begin{aligned} \frac{\delta\nu}{\nu} &= \frac{24\pi}{15} G\mu v_s \gamma_s (z_i + 1)^{1/2} (z(t) + 1)^{-1/2} \\ &\simeq 3 \times 10^{-5} (G\mu)_6 v\gamma(v), \end{aligned} \quad (29)$$

using $z_i + 1 = 10^3$ and $z + 1 = 30$ in the second line. Hence, an instrument with good frequency resolution is required to be able to measure the cosmic string wake signal at full strength. If the frequency resolution is worse than the above value, then the wake signal is still detectable, but with a reduced effective brightness.

The analysis presented up to this point has assumed that the initial thermal temperature T_g of the gas is negligible compared to the temperature acquired during infall. For small values of $G\mu$ this assumption will fail. In this case the wake will not experience shocks. The initial thermal velocities will dominate and will lead to a wider but more diffuse wake. The width in the presence of initial gas temperature compared to the width $w_{T_g=0}$

⁴ Note that T_γ is a decreasing function of time, whereas the wake temperature increases for a fixed wake.

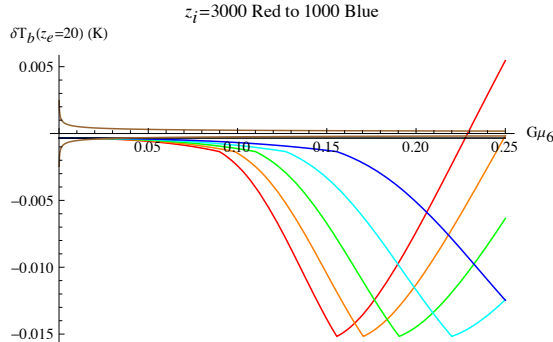


FIG. 7: Relative brightness temperature in degrees K induced by a cosmic string wake for various values of the formation redshift. The curves from left to right (in the region of low values of $G\mu$) correspond to $z_i = 3000, 2500, 2000, 1500$ and 1000 . The horizontal axis is the value of $G\mu$ in units of 10^{-6} . The two brown almost horizontal lines indicate the expected thermal noise per pixel of an experiment such as the SKA (the $G\mu$ dependence of the horizontal lines comes from the choice of the optimal pixel size as a function of $G\mu$ (see [49]).

for $T_g = 0$ is given by [49]

$$w(t)|_{T_K < T_g} = w(t)|_{T_g=0} \frac{T_g}{T_K}. \quad (30)$$

Since the hydrogen column density remains unchanged the temperature at a fixed point in the sky will decrease since the frequency dispersion increases.

In Figure 7 we show the brightness temperature excess as a function of $G\mu$ for various values of the formation redshift. For large values of $G\mu$, the relative brightness temperature is positive. For smaller values, it is an absorption effect. The kink point along each curve corresponds to the lowest value of $G\mu$ for which there is shock-heating. The (brown) almost horizontal lines on the graph correspond to the pixel by pixel sensitivity of an experiment such as the Square Kilometer Array (SKA), with a pixel size optimized as a function of $G\mu$ (see [49]). We see that the string signal is larger than the predicted noise level for values of $G\mu$ substantially smaller than the kink value.

Since the signal of a string wake has a very special pattern in position space, it is possible to search for this signal even if the relative brightness temperature at a fixed point in the sky is smaller than the pixel noise, in the same way that the line discontinuities caused by string segments in CMB temperature maps can be picked out for values of $G\mu$ where the pixel by pixel signal is hidden in the noise. As in the case of CMB temperature maps, it is important to use position space algorithms to analyze the maps. For an attempt to use Minkowski functionals to pick out string signals in 21cm redshift maps see [50].

Naturally, it is also possible to compute the power spectrum of the cosmic string wake signal in 21cm redshift maps. The angular power spectrum at a fixed value of the frequency has been computed in [51]. It is also

possible to compute the 21cm signal of a cosmic string loop. Since the overdensity in the region which accretes around the string loop is 64^5 for a loop compared to 4 for a wake (contraction occurs in all three dimensions), the induced brightness temperature is in fact even larger than for a string wake [42]. However, there are no special patterns which allow the string loop signal to be teased apart from background point sources. Hence, we consider it to be more promising to search for the signals of string wakes.

VI. CONCLUSIONS

I have discussed the search for cosmic string signals in new observational windows. There is good motivation for this work: detecting a cosmic string in cosmology would in itself be a great discovery which might lead to the solution of some outstanding problems in cosmology such as the origin of primordial magnetic fields which are coherent on galactic scales. Maybe more importantly, searching for cosmic strings in the sky is a way to probe particle physics beyond the Standard Model at energy scales which can never be reached in terrestrial accelerators.

Cosmic strings contribute to structure formation and hence leave imprints in the structure in the universe. However, the contribution of strings to the total power of cosmological perturbations is already bounded from above to be less than about 5% at the present time. The bulk of the power comes from almost Gaussian primordial fluctuations (here called Gaussian “noise”) such as those which could be generated by inflation or its alternatives.

The first main point to take away from this talk is that cosmic strings produce nonlinearities already at very high redshifts (whereas the Gaussian noise does not). Hence, the signatures of cosmic strings will be more pronounced at high redshifts. Hence, CMB anisotropy maps and 21cm redshift surveys are ideal windows to probe for strings.

The second main point is that cosmic strings produce fluctuations which are non-Gaussian. More specifically, string wakes induce signals with specific geometrical patterns in position space. Hence, better limits on cosmic strings can be achieved when analyzing the data in position space (e.g. with edge detection algorithms) rather than via power spectra computations.

Thirdly, the 21cm redshift survey window appears to be extremely promising. Improvements on the existing limits by several orders of magnitude should be possible.

There are other windows to probe cosmic strings. One is via gravitational waves. Oscillating cosmic string loops emit gravitational radiation [52]. A scaling network on strings will produce a scale-invariant spectrum of grav-

⁵ Assuming here that the initial translational motion of the string loop is negligible.

itational waves (see e.g. [53]). Cusps on cosmic strings may produce more distinctive signals [54]. However, it is expected that back-reaction effects (see e.g. [55]) could greatly reduce the gravitational wave signal of cusps, and hence limits on $G\mu$ derived from cusp signals should be taken with lots of grains of doubt.

Another window to probe cosmic strings is via high redshift galaxy surveys. The relative contribution of strings to correlation functions of nonlinear mass concentrations in the universe increases as the redshift grows. Hence, it is interesting to look for signals of cosmic strings in the high redshift galaxy distribution. Quite recently, the contribution of cosmic string loops to galaxy formation at high redshifts has been studied [56]. Correspond-

ing work on the effects of cosmic string wakes is ongoing at McGill.

Acknowledgments

I wish to thank Prof. Pauchy Hwang for the invitation to lecture at CosPA2012 and for his wonderful hospitality. I wish to thank all of my collaborators on the recent cosmic string work, and in particular Rebecca Danos for permission to use various figures drawn for [18, 35, 43], and Oscar Hernandez for permission to use Figure 7 which is taken from [49]. This research has been supported in part by an NSERC Discovery Grant and by funds from the Canada Research Chair program.

[1] T. W. B. Kibble, “Topology of Cosmic Domains and Strings,” J. Phys. A **9**, 1387 (1976).

[2] A. Vilenkin, “Cosmic Strings And Domain Walls,” Phys. Rept. **121**, 263 (1985);
A. Vilenkin and E.P.S. Shellard, *Cosmic Strings and other Topological Defects* (Cambridge Univ. Press, Cambridge, 1994);
M. B. Hindmarsh and T. W. B. Kibble, “Cosmic strings,” Rept. Prog. Phys. **58**, 477 (1995) [arXiv:hep-ph/9411342];
R. H. Brandenberger, “Topological defects and structure formation,” Int. J. Mod. Phys. A **9**, 2117 (1994) [arXiv:astro-ph/9310041].

[3] Y. B. Zeldovich, “Cosmological fluctuations produced near a singularity,” Mon. Not. Roy. Astron. Soc. **192**, 663 (1980);
A. Vilenkin, “Cosmological Density Fluctuations Produced By Vacuum Strings,” Phys. Rev. Lett. **46**, 1169 (1981) [Erratum-ibid. **46**, 1496 (1981)].

[4] R. Jeannerot, “A Supersymmetric SO(10) Model with Inflation and Cosmic Strings,” Phys. Rev. D **53**, 5426 (1996) [arXiv:hep-ph/9509365];
R. Jeannerot, J. Rocher and M. Sakellariadou, “How generic is cosmic string formation in SUSY GUTs,” Phys. Rev. D **68**, 103514 (2003) [arXiv:hep-ph/0308134].

[5] S. Sarangi and S. H. H. Tye, “Cosmic string production towards the end of brane inflation,” Phys. Lett. B **536**, 185 (2002) [arXiv:hep-th/0204074].

[6] R. H. Brandenberger and C. Vafa, “Superstrings In The Early Universe,” Nucl. Phys. B **316**, 391 (1989).;
A. Nayeri, R. H. Brandenberger and C. Vafa, “Producing a scale-invariant spectrum of perturbations in a Hagedorn phase of string cosmology,” Phys. Rev. Lett. **97**, 021302 (2006) [arXiv:hep-th/0511140];
R. H. Brandenberger, A. Nayeri, S. P. Patil and C. Vafa, “String gas cosmology and structure formation,” Int. J. Mod. Phys. A **22**, 3621 (2007) [hep-th/0608121];
R. H. Brandenberger, “String Gas Cosmology,” arXiv:0808.0746 [hep-th].

[7] T. W. B. Kibble, “Some Implications of a Cosmological Phase Transition,” Phys. Rept. **67**, 183 (1980);
T. W. B. Kibble, “Phase Transitions In The Early Universe,” Acta Phys. Polon. B **13**, 723 (1982).

[8] C. Dvorkin, M. Wyman and W. Hu, “Cosmic String constraints from WMAP and the South Pole Telescope,” Phys. Rev. D **84**, 123519 (2011) [arXiv:1109.4947 [astro-ph.CO]].

[9] C. L. Bennett *et al.*, “First Year Wilkinson Microwave Anisotropy Probe (WMAP) Observations: Preliminary Maps and Basic Results,” Astrophys. J. Suppl. **148**, 1 (2003) [arXiv:astro-ph/0302207].

[10] J. E. Ruhl *et al.* [The SPT Collaboration], “The South Pole Telescope,” Proc. SPIE Int. Soc. Opt. Eng. **5498**, 11 (2004) [arXiv:astro-ph/0411122].

[11] J. Urrestilla, N. Bevis, M. Hindmarsh and M. Kunz, “Cosmic string parameter constraints and model analysis using small scale Cosmic Microwave Background data,” JCAP **1112**, 021 (2011) [arXiv:1108.2730 [astro-ph.CO]].

[12] A. Kosowsky [the ACT Collaboration], “The Atacama Cosmology Telescope Project: A Progress Report,” New Astron. Rev. **50**, 969 (2006) [arXiv:astro-ph/0608549].

[13] L. Pogosian, S. H. H. Tye, I. Wasserman and M. Wyman, “Observational constraints on cosmic string production during brane inflation,” Phys. Rev. D **68**, 023506 (2003) [Erratum-ibid. D **73**, 089904 (2006)] [arXiv:hep-th/0304188];
M. Wyman, L. Pogosian and I. Wasserman, “Bounds on cosmic strings from WMAP and SDSS,” Phys. Rev. D **72**, 023513 (2005) [Erratum-ibid. D **73**, 089905 (2006)] [arXiv:astro-ph/0503364];
A. A. Fraisse, “Limits on Defects Formation and Hybrid Inflationary Models with Three-Year WMAP Observations,” JCAP **0703**, 008 (2007) [arXiv:astro-ph/0603589];
U. Seljak, A. Slosar and P. McDonald, “Cosmological parameters from combining the Lyman-alpha forest with CMB, galaxy clustering and SN constraints,” JCAP **0610**, 014 (2006) [arXiv:astro-ph/0604335];
R. A. Battye, B. Garbrecht and A. Moss, “Constraints on supersymmetric models of hybrid inflation,” JCAP **0609**, 007 (2006) [arXiv:astro-ph/0607339];
R. A. Battye, B. Garbrecht, A. Moss and H. Stoica, “Constraints on Brane Inflation and Cosmic Strings,” JCAP **0801**, 020 (2008) [arXiv:0710.1541 [astro-ph]];
N. Bevis, M. Hindmarsh, M. Kunz and J. Urrestilla, “CMB power spectrum contribution from cosmic strings using field-evolution simulations of the Abelian Higgs model,” Phys. Rev. D **75**, 065015 (2007) [arXiv:astro-

ph/0605018];
 N. Bevis, M. Hindmarsh, M. Kunz and J. Urrestilla, “Fitting CMB data with cosmic strings and inflation,” Phys. Rev. Lett. **100**, 021301 (2008) [astro-ph/0702223 [ASTRO-PH]];
 R. Battye and A. Moss, “Updated constraints on the cosmic string tension,” Phys. Rev. D **82**, 023521 (2010) [arXiv:1005.0479 [astro-ph.CO]].

[14] R. H. Brandenberger, A. -C. Davis and M. Hindmarsh, “Baryogenesis from collapsing topological defects,” Phys. Lett. B **263**, 239 (1991);
 R. H. Brandenberger, A. -C. Davis and M. Trodden, “Cosmic strings and electroweak baryogenesis,” Phys. Lett. B **335**, 123 (1994) [hep-ph/9403215];
 R. H. Brandenberger, A. -C. Davis, T. Prokopec and M. Trodden, “Local and nonlocal defect mediated electroweak baryogenesis,” Phys. Rev. D **53**, 4257 (1996) [hep-ph/9409281].

[15] R. H. Brandenberger and X. -m. Zhang, “Anomalous global strings and primordial magnetic fields,” Phys. Rev. D **59**, 081301 (1999) [hep-ph/9808306].

[16] J. H. MacGibbon and R. H. Brandenberger, “Gamma-ray signatures from ordinary cosmic strings,” Phys. Rev. D **47**, 2283 (1993) [astro-ph/9206003];
 P. Bhattacharjee, C. T. Hill and D. N. Schramm, “Grand unified theories, topological defects and ultrahigh-energy cosmic rays,” Phys. Rev. Lett. **69**, 567 (1992);
 P. Bhattacharjee and N. C. Rana, “Ultrahigh-energy Particle Flux From Cosmic Strings,” Phys. Lett. B **246**, 365 (1990);
 J. H. MacGibbon and R. H. Brandenberger, “High-energy Neutrino Flux From Ordinary Cosmic Strings,” Nucl. Phys. B **331**, 153 (1990).

[17] R. Brandenberger, Y. -F. Cai, W. Xue and X. -m. Zhang, “Cosmic Ray Positrons from Cosmic Strings,” arXiv:0901.3474 [hep-ph].

[18] R. H. Brandenberger, R. J. Danos, O. F. Hernandez and G. P. Holder, “The 21 cm Signature of Cosmic String Wakes,” JCAP **1012**, 028 (2010) [arXiv:1006.2514 [astro-ph.CO]].

[19] N. Kaiser and A. Stebbins, “Microwave Anisotropy Due To Cosmic Strings,” Nature **310**, 391 (1984).

[20] J. R. Gott, III, “Gravitational lensing effects of vacuum strings: Exact solutions,” Astrophys. J. **288**, 422 (1985).

[21] J. Silk and A. Vilenkin, “Cosmic Strings And Galaxy Formation,” Phys. Rev. Lett. **53**, 1700 (1984);
 M. Rees, “Baryon concentrations in string wakes at $z \geq 200$: implications for galaxy formation and large-scale structure,” Mon. Not. R. astr. Soc. **222**, 27p (1986);
 T. Vachaspati, “Cosmic Strings and the Large-Scale Structure of the Universe,” Phys. Rev. Lett. **57**, 1655 (1986);
 A. Stebbins, S. Veeraraghavan, R. H. Brandenberger, J. Silk and N. Turok, “Cosmic String Wakes,” Astrophys. J. **322**, 1 (1987).

[22] L. Dolan and R. Jackiw, “Symmetry Behavior at Finite Temperature,” Phys. Rev. D **9**, 3320 (1974).

[23] D. A. Kirzhnits and A. D. Linde, “Macroscopic Consequences of the Weinberg Model,” Phys. Lett. B **42**, 471 (1972).

[24] R. H. Brandenberger, “Quantum Field Theory Methods and Inflationary Universe Models,” Rev. Mod. Phys. **57**, 1 (1985).

[25] N. Turok and R. H. Brandenberger, “Cosmic Strings And The Formation Of Galaxies And Clusters Of Galaxies,” Phys. Rev. D **33**, 2175 (1986);
 H. Sato, “Galaxy Formation by Cosmic Strings,” Prog. Theor. Phys. **75**, 1342 (1986);
 A. Stebbins, “Cosmic Strings and Cold Matter”, Ap. J. (Lett.) **303**, L21 (1986).

[26] E. P. S. Shellard, “Cosmic String Interactions,” Nucl. Phys. B **283**, 624 (1987).

[27] A. Albrecht and N. Turok, “Evolution Of Cosmic Strings,” Phys. Rev. Lett. **54**, 1868 (1985);
 D. P. Bennett and F. R. Bouchet, “Evidence For A Scaling Solution In Cosmic String Evolution,” Phys. Rev. Lett. **60**, 257 (1988);
 B. Allen and E. P. S. Shellard, “Cosmic String Evolution: A Numerical Simulation,” Phys. Rev. Lett. **64**, 119 (1990);
 C. Ringeval, M. Sakellariadou and F. Bouchet, “Cosmological evolution of cosmic string loops,” JCAP **0702**, 023 (2007) [arXiv:astro-ph/0511646];
 V. Vanchurin, K. D. Olum and A. Vilenkin, “Scaling of cosmic string loops,” Phys. Rev. D **74**, 063527 (2006) [arXiv:gr-qc/0511159];
 J. J. Blanco-Pillado, K. D. Olum and B. Shlaer, “Large parallel cosmic string simulations: New results on loop production,” Phys. Rev. D **83**, 083514 (2011) [arXiv:1101.5173 [astro-ph.CO]].

[28] J. Magueijo, A. Albrecht, D. Coulson and P. Ferreira, “Doppler peaks from active perturbations,” Phys. Rev. Lett. **76**, 2617 (1996) [arXiv:astro-ph/9511042];
 U. L. Pen, U. Seljak and N. Turok, “Power spectra in global defect theories of cosmic structure formation,” Phys. Rev. Lett. **79**, 1611 (1997) [arXiv:astro-ph/9704165];
 L. Perivolaropoulos, “Spectral Analysis Of Microwave Background Perturbations Induced By Cosmic Strings,” Astrophys. J. **451**, 429 (1995) [arXiv:astro-ph/9402024].

[29] J. H. Traschen, N. Turok and R. H. Brandenberger, “Microwave Anisotropies from Cosmic Strings,” Phys. Rev. D **34**, 919 (1986);
 R. H. Brandenberger and N. Turok, “Fluctuations From Cosmic Strings And The Microwave Background,” Phys. Rev. D **33**, 2182 (1986).

[30] P. D. Mauskopf *et al.* [Boomerang Collaboration], “Measurement of a Peak in the Cosmic Microwave Background Power Spectrum from the North American test flight of BOOMERANG,” Astrophys. J. **536**, L59 (2000) [arXiv:astro-ph/9911444].

[31] A. Vilenkin, “Gravitational Field Of Vacuum Domain Walls And Strings,” Phys. Rev. D **23**, 852 (1981);
 R. Gregory, “Gravitational Stability of Local Strings,” Phys. Rev. Lett. **59**, 740 (1987).

[32] J. C. R. Magueijo, “Inborn metric of cosmic strings,” Phys. Rev. D **46**, 1368 (1992).

[33] L. Perivolaropoulos, “COBE versus cosmic strings: An Analytical model,” Phys. Lett. B **298**, 305 (1993) [arXiv:hep-ph/9208247];
 L. Perivolaropoulos, “Statistics of microwave fluctuations induced by topological defects,” Phys. Rev. D **48**, 1530 (1993) [arXiv:hep-ph/9212228].

[34] J. Canny, “A computational approach to edge detection”, IEEE Trans. Pattern Analysis and Machine Intelligence **8**, 679 (1986).

[35] R. J. Danos and R. H. Brandenberger, “Canny Algorithm, Cosmic Strings and the Cosmic Microwave

Background,” Int. J. Mod. Phys. D **19**, 183 (2010) [arXiv:0811.2004 [astro-ph]].

[36] S. Amsel, J. Berger and R. H. Brandenberger, “Detecting Cosmic Strings in the CMB with the Canny Algorithm,” JCAP **0804**, 015 (2008) [arXiv:0709.0982 [astro-ph]].

[37] A. Stewart and R. Brandenberger, “Edge Detection, Cosmic Strings and the South Pole Telescope,” JCAP **0902**, 009 (2009) [arXiv:0809.0865 [astro-ph]].

[38] Y. .B. Zeldovich, “Gravitational instability: An Approximate theory for large density perturbations,” Astron. Astrophys. **5**, 84 (1970).

[39] A. Sornborger, R. H. Brandenberger, B. Fryxell and K. Olson, “The Structure of cosmic string wakes,” Astrophys. J. **482**, 22 (1997) [astro-ph/9608020].

[40] R. H. Brandenberger, N. Kaiser and N. Turok, “Dissipationless Clustering Of Neutrinos Around A Cosmic String Loop,” Phys. Rev. D **36**, 2242 (1987); R. H. Brandenberger, N. Kaiser, D. N. Schramm and N. Turok, “Galaxy and Structure Formation with Hot Dark Matter and Cosmic Strings,” Phys. Rev. Lett. **59**, 2371 (1987).

[41] R. H. Brandenberger, L. Perivolaropoulos and A. Stebbins, “Cosmic Strings, Hot Dark Matter And The Large Scale Structure Of The Universe,” Int. J. Mod. Phys. A **5**, 1633 (1990); L. Perivolaropoulos, R. H. Brandenberger and A. Stebbins, “Dissipationless Clustering Of Neutrinos In Cosmic String Induced Wakes,” Phys. Rev. D **41**, 1764 (1990).

[42] M. Pagano and R. Brandenberger, “The 21cm Signature of a Cosmic String Loop,” JCAP **1205**, 014 (2012) [arXiv:1201.5695 [astro-ph.CO]].

[43] R. J. Danos, R. H. Brandenberger and G. Holder, “A Signature of Cosmic Strings Wakes in the CMB Polarization,” Phys. Rev. D **82**, 023513 (2010) [arXiv:1003.0905 [astro-ph.CO]].

[44] O. Dore, G. Holder, M. Alvarez, I. T. Iliev, G. Mellema, U. -L. Pen and P. R. Shapiro, “The Signature of Patchy Reionization in the Polarization Anisotropy of the CMB,” Phys. Rev. D **76**, 043002 (2007) [astro-ph/0701784 [ASTRO-PH]].

[45] R. H. Brandenberger, “Is the Spectrum of Gravitational Waves the ‘Holy Grail’ of Inflation?,” arXiv:1104.3581 [astro-ph.CO].

[46] R. H. Brandenberger, A. Nayeri, S. P. Patil and C. Vafa, “Tensor Modes from a Primordial Hagedorn Phase of String Cosmology,” Phys. Rev. Lett. **98**, 231302 (2007) [hep-th/0604126].

[47] R. Khatri and B. D. Wandelt, “Cosmic (super)string constraints from 21 cm radiation,” Phys. Rev. Lett. **100**, 091302 (2008) [arXiv:0801.4406 [astro-ph]]; A. Berndsen, L. Pogosian and M. Wyman, “Correlations between 21 cm Radiation and the CMB from Active Sources,” arXiv:1003.2214 [astro-ph.CO].

[48] S. Furlanetto, S. P. Oh and F. Briggs, “Cosmology at Low Frequencies: The 21 cm Transition and the High-Redshift Universe,” Phys. Rept. **433**, 181 (2006) [arXiv:astro-ph/0608032].

[49] O. F. Hernandez and R. H. Brandenberger, “The 21 cm Signature of Shock Heated and Diffuse Cosmic String Wakes,” JCAP **1207**, 032 (2012) [arXiv:1203.2307 [astro-ph.CO]].

[50] E. McDonough and R. H. Brandenberger, “Searching for Signatures of Cosmic String Wakes in 21cm Redshift Surveys using Minkowski Functionals,” arXiv:1109.2627 [astro-ph.CO].

[51] O. F. Hernandez, Y. Wang, R. Brandenberger and J. Fong, “Angular 21 cm Power Spectrum of a Scaling Distribution of Cosmic String Wakes,” JCAP **1108**, 014 (2011) [arXiv:1104.3337 [astro-ph.CO]].

[52] T. Vachaspati and A. Vilenkin, “Gravitational Radiation from Cosmic Strings,” Phys. Rev. D **31**, 3052 (1985); R. L. Davis, “Nucleosynthesis Problems for String Models of Galaxy Formation”, Phys. Lett. **B 161**, 285 (1985).

[53] R. H. Brandenberger, A. Albrecht and N. Turok, “Gravitational Radiation From Cosmic Strings And The Microwave Background,” Nucl. Phys. B **277**, 605 (1986).

[54] T. Damour and A. Vilenkin, “Gravitational wave bursts from cosmic strings,” Phys. Rev. Lett. **85**, 3761 (2000) [gr-qc/0004075].

[55] R. H. Brandenberger, “On The Decay Of Cosmic String Loops,” Nucl. Phys. B **293**, 812 (1987).

[56] B. Shlaer, A. Vilenkin and A. Loeb, “Early structure formation from cosmic string loops,” JCAP **1205**, 026 (2012) [arXiv:1202.1346 [astro-ph.CO]].